CHAPTER- 2

Instrumentation and Experimental Techniques

This chapter provides a brief explanation of the experimental setup and characterization techniques we have used to investigate the structural, morphological, and electrochemical properties of synthesized nanomaterials. Comprehensive characterization of nanomaterials and their nanocomposites is achieved through a variety of instrumental techniques, such as X-ray diffractometer (XRD), X-ray photoelectron spectroscopy (XPS), scanning electron microscopy (SEM), transmission electron microscopy (TEM), and atomic force microscopy (AFM). The cyclic voltammetry (CV), differential pulse voltammetry (DPV), amperometry, and electrochemical impedance spectroscopy (EIS) techniques have been used for electrochemical sensing of various analytes such as ascorbic acid, dopamine, and NADH. This chapter covers the fundamental background of all of the techniques we have used.

2.1 Characterization techniques

2.1.1 X-ray diffractometry (XRD)

X-ray diffractometry is a versatile method that offers comprehensive details on the crystallographic structure and chemical makeup of both natural and artificial materials [1,2]. XRD analysis is performed to analyze the phase formation and crystallinity of synthesized nanomaterial. The determination and characterization of compounds based on their diffraction pattern is the main use of this method. In X-ray diffraction, the uniform spacing between atoms in a crystal results in an interference pattern of the waves in an incoming X-ray beam [3]. The XRD pattern is produced by constructive interference between monochromatic X-rays and a crystalline sample [4]. The sample is subjected to strong monochromatic X-ray energy, which combines with it according to Bragg's Law ($2dsin\theta = n\lambda$), this results in diffracted beams and constructive interference (Figure 2.1

(a)). Bragg's law describes the link between X-ray wavelength (λ), diffraction angle (θ), and lattice spacing (d) in crystalline samples. When diffracted X-rays from the sample are passed through the detectors, all potential lattice diffraction orientations may be achieved by scanning the sample across a range of 2θ angles. Afterward, using these diffraction peaks (patterns), a set of precise d-spacing is determined for every sample. By comparing the d-spacing with a standardized reference pattern, we may subsequently ascertain the material's phase and crystallographic structure.

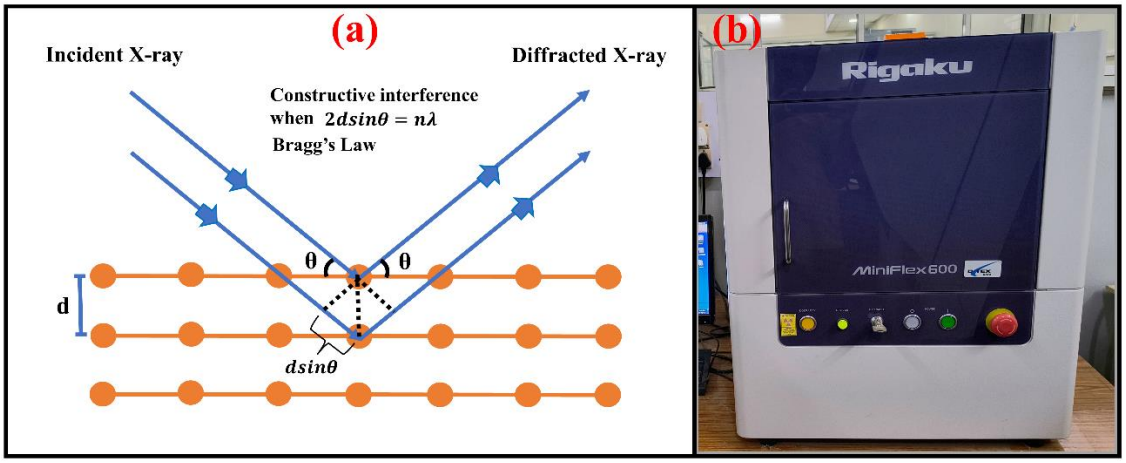

Figure 2.1 (a) Schematic diagram for X-ray diffraction (b) Miniflex 600 X-ray diffractometer (Rigaku, Courtesy CIFC IIT BHU).

We have used an X-ray diffractometer (Rigaku Miniflex 600) with Cu-Kα (λ=1.5405 Å) to characterize the synthesized material (Figure 2.1(b)). The diffractometer was calibrated utilizing silica powder. Single-crystal silicon was utilized as a reference to determine the exact value of 2θ for the calculation of the quasi-lattice parameter. The XRD spectrum has been obtained involving 10°-80° in 2θ utilizing a step size of 3°/min (depending on the requirement these parameters may vary).

2.1.2 Scanning electron microscopy (SEM)

Scanning electron microscopy is a powerful technique used for analyzing the size, shape, and morphologies of synthesized nanoparticles, providing high-resolution pictures of the expected study material [5]. It provides information on the topography, chemical compositions, and microstructure morphologies of both synthesized and naturally occurring materials [6]. The versatility of SEM makes it appropriate for a wide range of scientific, research, industrial, and commercial applications, such as biological science, forensics, medical science, electronics, materials science, etc.

In SEM, electrons are generated from heating tungsten filaments or single crystals of lanthanum hexaboride (LaB_6), which are then accelerated by voltages typically between 20 and 30 kV [7]. Before use sample is coated with gold metal to make the surface more conductive. The collection of signals resulting from the interaction between the electron beam and sample is necessary for the generation of images in the SEM. The SEM device we have utilized for the characterization of nanomaterials is displayed in (Figure 2.2).

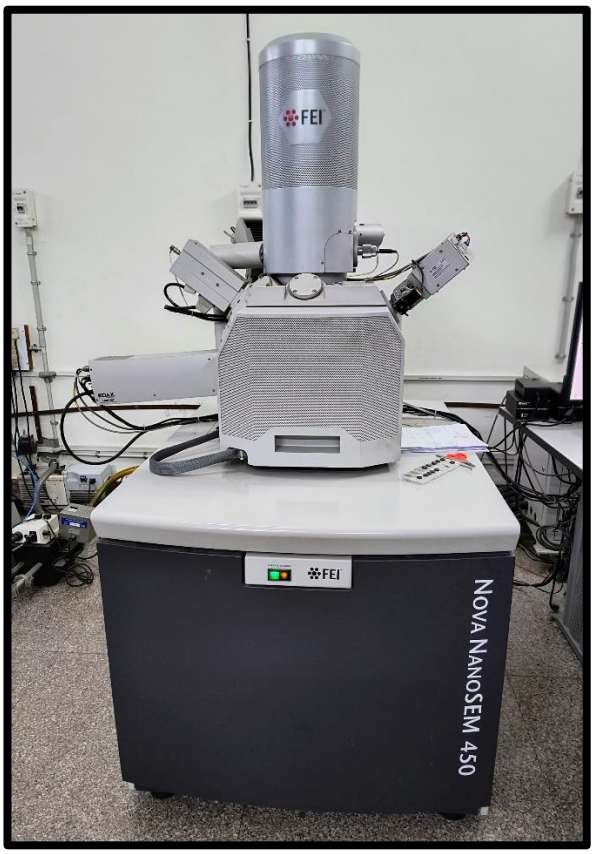

Figure 2.2 Scanning electron microscopy (FEI Nova Nano SEM 450, Courtesy CIFC IIT BHU).

2.1.3 Energy dispersive X-ray spectroscopy (EDX)

Energy dispersive X-ray (EDX) analysis is also known as energy dispersive X-ray spectroscopy (EDS). It is a method used for determining the material's chemical composition by analyzing the energy of X-rays emitted by an electron beam [8]. In this thesis, SEM-EDX was performed to know the distribution of elements present on the surface.

Working principle: The electron beam strikes the inner shell of an atom and an electron is ejected creating a positively charged hole. The positively charged hole generated gets filled up by the outer shell electrons by releasing energy in the form of an X-ray [9]. The

energy spectrum of X-rays is unique to each element and depends on the shell from which electrons move into the holes, allowing the elements in the sample to be identified. (Figure 2.3) shows the block diagram of the working principle of EDX.

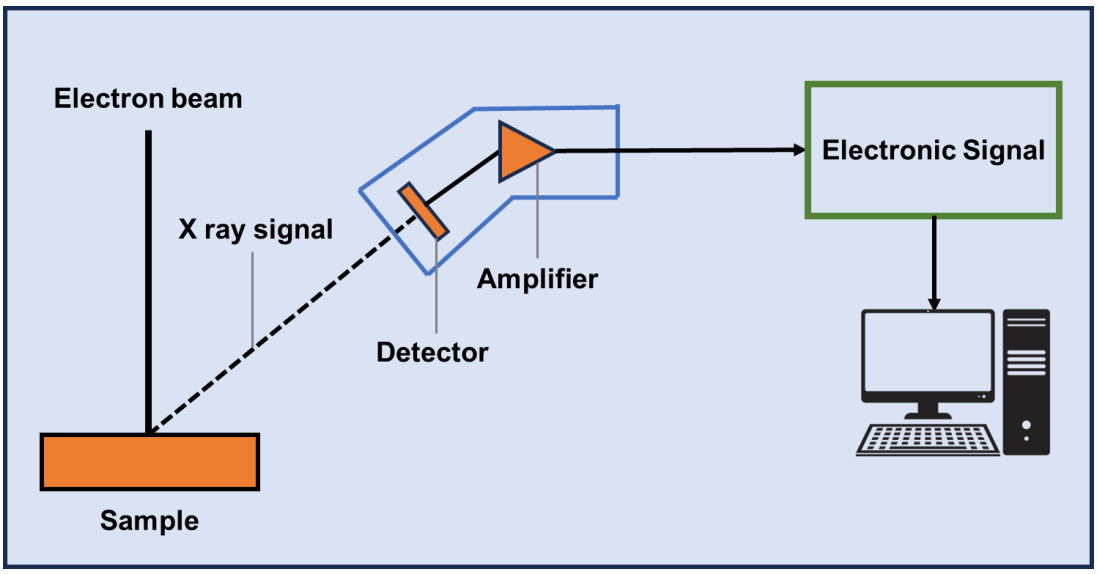

Figure 2.3 Schematic diagram of Energy dispersive X-ray spectrophotometer (EDX)

2.1.4 Transmission electron microscopy (TEM)

Transmission electron microscopy is one of the most effective characterization techniques which is defined as the study of the interaction between an extremely thin, transparent sample (less than 100 nm) and a high-energy electron beam (between 60 to 400 keV) [10]. This interaction produces several distinct signals. In the transmission electron microscope, the transmitted signals developed during the electron beam and sample interaction formed a highly resolved and enlarged picture of the specimen [11]. TEM techniques are capable of providing information about a sample's nanostructure, chemical constituents, and electronic properties at the nanoscale [12]. In this thesis, TEM is performed to obtain detailed information about the internal structure

such as the size, and shape of nanomaterials. To determine the particle size histogram from a TEM image we have used ImageJ software. For the structural characterization of synthesized nanomaterials, we have used a transmission electron microscope (TEM)-FEI-Tecnai 20 U Twin with EDX and Tecnai 20 G2, operated at 200 KeV illustrated in (Figure 2.4).

Figure 2.4 Transmission electron microscopy with EDX (FEI, TECHNAI G2 20 TWIN, Courtesy CIFC IIT BHU).

2.1.5 Atomic force microscopy (AFM)

The atomic force microscope is a type of scanning probe microscope that uses interactions between a tip and a sample surface to create a topographical picture of the surface of the sample. Although this method depends on the conductive samples, the AFM allows also the use of non-conductive samples. In 1987, the inventors were awarded the Nobel Prize in Physics for their achievements. In general, this technique is used to examine the properties of grains, phases, and surface layers in many materials, including metallic, ceramic, polymer-based, organic, and inorganic composites [13]. In this thesis, AFM is performed to analyze grain size. The grain size histogram from an atomic force microscopy image was determined by using the line cut method on Nova Px 3.4 software.

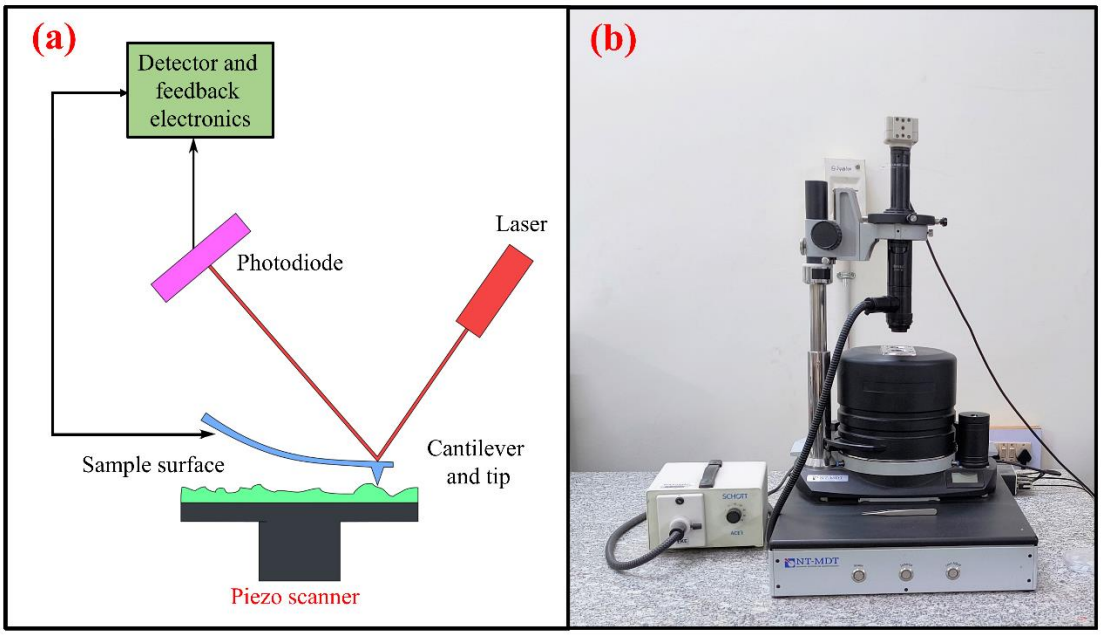

Figure 2.5 (a) Schematic representation of atomic force microscope **(b)** Scanning probe microscopy (NTEGRA Prima Courtesy CIFC IIT BHU).

In atomic force microscopy, a laser beam is reflected from its point of origin off the cantilever and towards a four-quadrant photodetector (Figure 2.5 (a)). A four-quadrant

detector allows for the detection of interatomic forces in both the lateral and vertical directions. As the AFM interacts with the sample the position and intensity of the reflected beam are recorded on the detector. The information recorded by this detector can be used differently depending on the operation mode of the AFM. AFM captures a three-dimensional picture of the sample's surface topography while applying a steady force (nano Newton range) [14,15]. For the characterization of synthesized palladium nanoparticles, we have used atomic force microscopy (Model: NTEGRA Prima, Company: NT-MDT Service & Logistics Ltd.) as shown in (Figure 2.5 (b)).

2.1.6 X-ray photoelectron spectroscopy (XPS)

X-ray photoelectron spectroscopy is a powerful surface analysis technique used to investigate the elemental composition, chemical state, and electronic structure of materials. In XPS, the conventional methodology for conducting spectroscopic surface analysis involves subjecting the sample to an incident beam consisting of photons and electrons. The interaction between the primary beam and the surface leads to the generation of a secondary beam originating from the substrate, which is subsequently detected and measured by the spectrometer [16] (Figure 2.6 (a)). This method involves bombarding the material surface with X-rays and measuring the kinetic energy of the expelled electrons [17]. XPS instrument uses Al Kα rays and can detect components within a few nanometers of the sample surface. The two main characteristics of this approach are its surface sensitivity and its capacity to study the chemical and oxidation states of the components in the sample [18]. By using this technique every element can be identified except hydrogen and helium. The graph of the XPS spectrum is plotted between intensity (count/sec) versus binding energy (eV). Generally, the XPS survey

spectrum scan between the binding energy 0 to 1200 eV. The XPS spectra were fitted using peak 41 software. In the current thesis, for the XPS analysis of synthesized nanomaterials and their composites, we have used an X-ray photoelectron spectrometer (Model: K-alpha, Company: Thermo Fischer Scientific) as shown in (Figure 2.6 (b)).

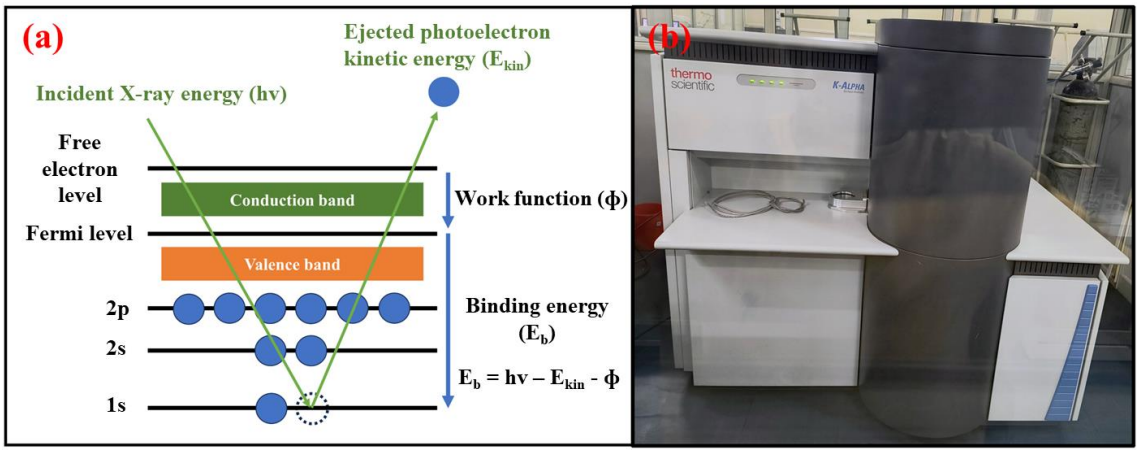

Figure 2.6 (a) Schematic representation of X-ray photon spectroscopy (b) X-ray photoelectron spectrometer (K-alpha model of Thermo Fischer Scientific, Courtesy CIFC IIT BHU).

2.1.7 Electrochemical Characterizations

The current study demonstrates electrochemical characterizations of the fabricated electrodes and investigates their electrochemical response through the utilization of cyclic voltammetry, differential pulse voltammetry, amperometry, and electrochemical impedance spectroscopy on CHI 660E Inc., Texas, USA as depicted in Figure 2.7. These analyses were performed utilizing a three-electrode assembly with a working volume of 2 mL phosphate buffer solution (pH 7.0) and involved the measurement of current potential.

The three electrodes used are the working electrode, reference electrode (Ag/AgCl), and counter electrode (Platinum foil). The first electrode is the working electrode at which the

redox reaction takes place. The counter electrode is the second electrode, which is essential for completing the electric circuit. The third electrode is known as the reference electrode, and its potential is measured with respect to the standard hydrogen electrode (0.00 V). It is used to measure the potential of the working electrode relative to the reference electrode, regardless of the analyte concentration. The electrolyte filled in the Ag/AgCl reference electrode (RE 1B ALS Co. Ltd, Japan) is 3 M sodium chloride (NaCl). The electrode's potential is calculated from the activity of the chloride ion, not its concentration.

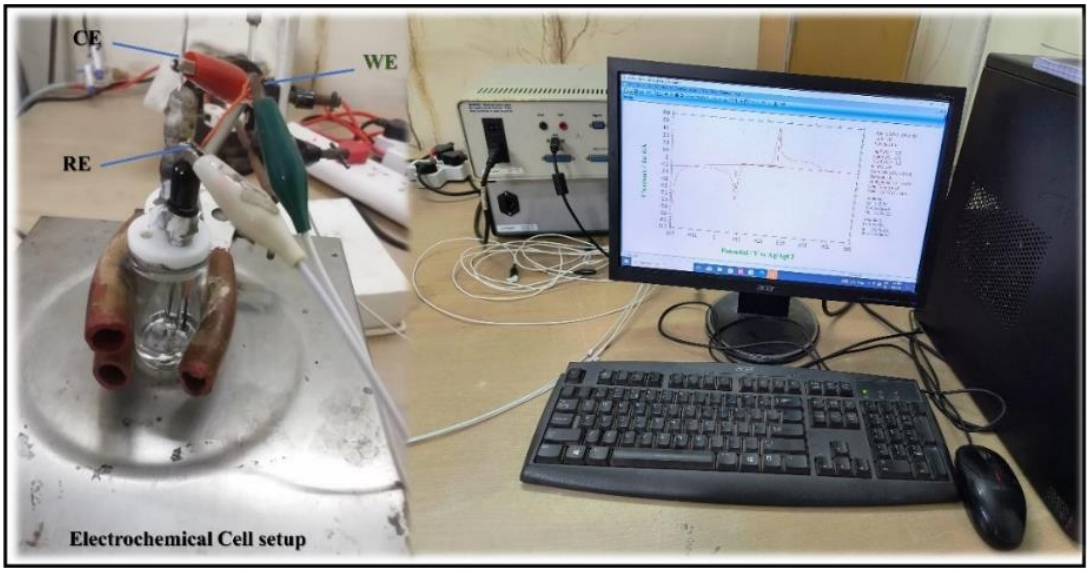

Figure 2.7 CHI 608E Inc., Texas, USA with three-electrode electrochemical cell setup.

2.1.7.1 Cyclic voltammetry (CV)

Cyclic voltammetry is a typical and widely used measuring technique for determining the redox activity of any substance. It is an electrochemical technique performed by varying the potential of the working electrode linearly with time while maintaining a constant scan rate [19,20]. CV is particularly suitable for analyzing redox-active biomolecules

such as ascorbic acid, dopamine, and NADH because it provides direct information about the redox potentials, reversibility of the reactions, and electron transfer kinetics. CV can provide insights into whether the reaction is diffusion-controlled or surface-controlled. So, CV is important for understanding the electrochemical behavior of ascorbic acid, dopamine, and NADH which involves a fast electron transfer process. The typically used CV graph is depicted in Figure 2.8, where the reduction peak is associated with the bottom half (negative current), and the oxidation peak is connected to the upper half (positive current). It is also a valuable method for studying chemical processes in catalysis that are initiated by electron transport.

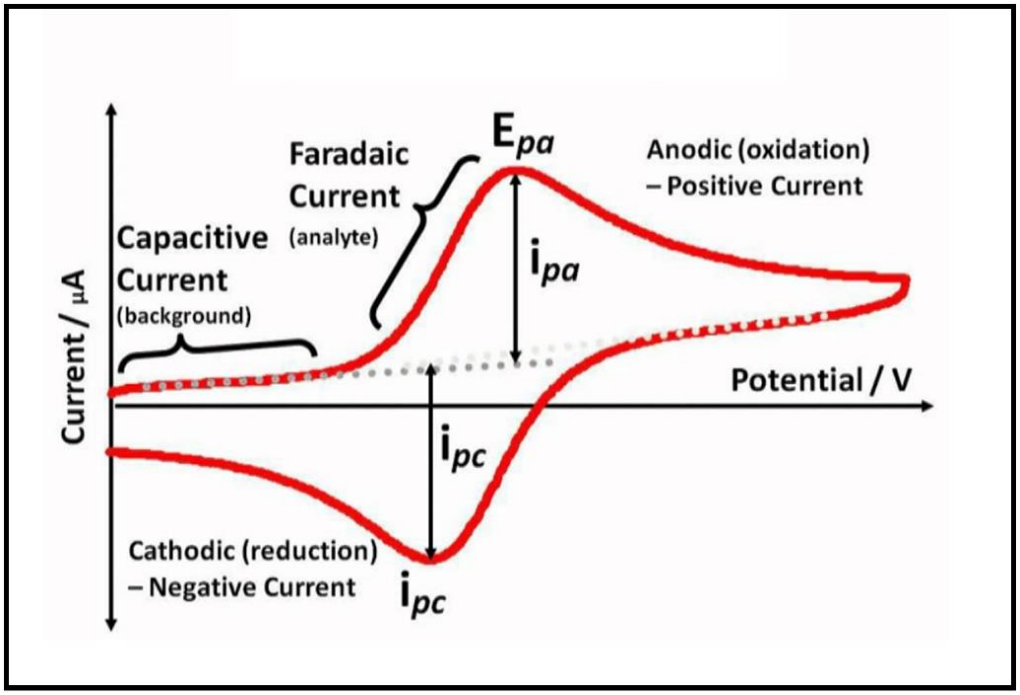

Figure 2.8 Figure of cyclic voltammogram (Courtesy: Wikimedia Commons).

The applied potential's speed is governed by the scan rate in the CV experiment. Thus, the famous Randles-Sevcik equation states that the peak current (I_p) is dependent on the

scan rate [21]. This equation is used when the reaction is electrochemically reversible and the product and reactant both are soluble. It is not valid when the catalyst undergoes dynamic dissolution.

$$\boldsymbol{I_p = (2 \cdot 69 * 10^5) n^{3/2} A D^{1/2} \nu^{1/2} C_0} \quad (2.1)$$

Where I_p is peak current, n is the number of electrons that participate during the redox reaction, A is the electroactive surface area of the electrode, D is diffusion coefficient, υ is scan rate, and C_0 is the concentration of the electroactive analyte. Equation 2.1 shows that peak current is directly proportional to the square root of the scan rate.

In electrochemical reactions, kinetics play an important role in determining the electron transport rate. In a reversible reaction, the transfer of electrons between the electrode and the analyte proceeds quickly enough to establish equilibrium almost instantly. In a reversible process, the electron transfer rate is much greater than the mass transfer rate of diffusion while in an irreversible process, the electron transfer rate is much less than the mass transfer rate of diffusion. The cyclic voltammogram of a reversible redox process is analyzed using the following variables:

1. The formal potential ($E^{0'}$) can be determined from the peak potentials in cyclic voltammetry using the equation: $E^{0'} = (E_{pc} + E_{pa})/2$.
2. The peak potential difference [$\Delta E_p = E_{pc} - E_{pa}$] = 59.2/n mV at 25°C
3. The ratio of peak current I = I_{pa}/I_{pc} = 1 (for all scan rates)

2.1.7.2 Differential pulse voltammetry (DPV)

Differential pulse voltammetry (DPV) is a widely used electrochemical technique for the qualitative and quantitative analysis of electroactive species in solution. It provides high sensitivity and resolution, ideal for quantitative analysis of low-concentration analytes. It is a method that includes applying very small amplitude potential pulses (10-100 mV) to a linear ramp potential and brief pulses (17 ms) are superimposed on a staircase-wave form [22]. In DPV, a base potential value is applied to the electrode at which there is no faradaic reaction occurs. The base potential increases in equal increments between pulses [23]. The current is measured immediately before the pulse application (I_1) and after the pulse (I_2) as shown in Figure 2.9 (a). The direct current ramp is responsible for the first current, the potential pulse's current is reflected by the difference (I_2-I_1), and the signal in DPV is the product of the difference between the signal immediately preceding the pulse and the signal at its conclusion (Figure 2.9 (b)). To collect the DPV data we have used 0.05 V pulse amplitude, 0.2 sec pulse period, 0.0167 sec sampling width, and 0.05 sec pulse width.

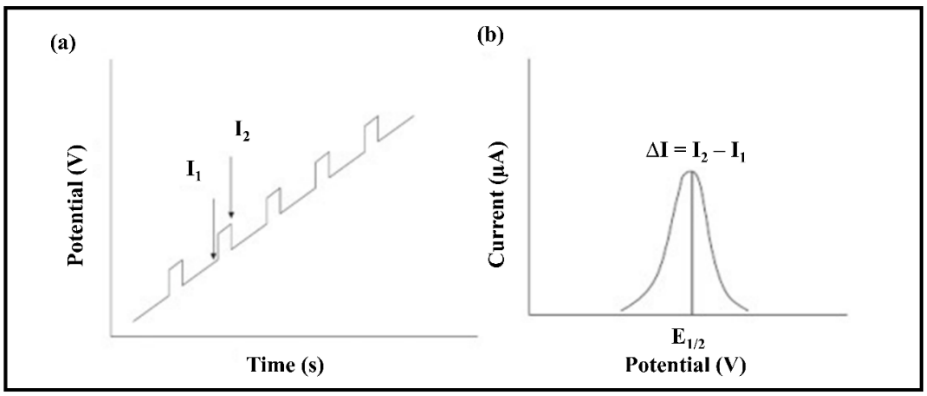

Figure 2.9 (a) Applied waveform for DPV (b) Typical voltammogram response obtained in DPV [24].

In DPV the graph is plotted between current versus applied potential and the current is directly proportional to the concentration of the corresponding analyte. The most significant advantage of DPV is increased sensitivity due to reduced capacitive current. The smaller step sizes in the DPV approach result in narrow peaks, so DPV can be used to identify analytes with similar oxidation potentials.

2.1.7.3 Amperometry

Amperometry is an electroanalytical method that measures current with respect to time using a constant anodic or cathodic potential. It is used for real-time monitoring of biomolecules (e.g., ascorbic acid, dopamine, NADH, etc.) with high sensitivity, especially in dynamic environments. The Cottrell equation predicts that current is directly proportional to the concentration of electroactive molecules [25] as shown in the equation (2.2). The Cottrell equation is valid for a controlled potential experiment, such as chronoamperometry, where the potential is a step function in time. The Cottrell equation is applicable for planar electrodes. It can also be derived for other geometries using Fick's second law of diffusion and the corresponding Laplace operator and boundary conditions.

$$\boldsymbol{I = \frac{nFA(D)^{\frac{1}{2}}C}{(\pi t)^{1/2}}} \qquad (2.2)$$

Where I is the current (A), n is the number of electrons during the electrochemical reaction, F is the Faraday constant (C/mol), A is the area of the electrode (cm^2), D is the diffusion coefficient of the electroactive species (cm^2/s), C is the concentration of electroactive species, and t is the time (s). The magnitude of the current is proportional to the concentration of oxidized or reduced electroactive substances. Thus, the

amperometric technique provides a simple and sensitive methodology for identifying electroactive species in solution by using a constant potential and convection.

2.1.7.4 Electrochemical impedance spectroscopy (EIS)

Electrochemical impedance spectroscopy is a well-known analytical technique used for the analysis of electrochemical systems by providing a very small alternative current voltage signal based on the frequency of the amplitude signal. The AC signal is scanned across a wide frequency range to generate impedance spectra of the electrochemical cell under study [26]. It provides information about the processes occurring at the electrode-electrolyte interface, such as charge transfer reactions, double-layer capacitance, mass transport, and adsorption/desorption phenomena [27]. EIS is particularly useful for analyzing ascorbic acid, dopamine, and NADH because it provides detailed information about charge transfer kinetics and electrode surface interactions. EIS captures details regarding resistance during electron transport processes by measuring impedance over the 1 Hz to 1000 kHz frequency range. It is a highly sensitive technique and can identify analyte concentrations faster than traditional methods that's why EIS is more suitable for sensing applications.

The impedance data obtained from EIS experiments are typically represented in Nyquist plots or Bode plots. The EIS data was fitted on R(CR)W circuit by using ZSimpWin software. In a Nyquist plot, the data is plotted between the real part of the impedance (Z') versus the imaginary part of the impedance (-Z''). The resulting plot often resembles a semicircle at high frequencies, the diameter of which provides information about the charge transfer resistance at the electrode-electrolyte interface, while the linear part at low

frequency shows the diffusion-controlled processes [28]. EIS has several advantages over other electrochemical techniques. It provides detailed information about both kinetic and transport processes within the system. Therefore, EIS may be utilized in several critical biological sensing and diagnostic fields.

2.1.7.5 Optimization of experimental conditions

Optimization of experimental conditions during electrochemical sensing of biomolecules is crucial for enhancing sensitivity, selectivity, stability, and reproducibility. The key variables that influence electrochemical responses include potential window, scan rate, and step size. These parameters directly affect the electron transfer kinetics, the diffusion layer's thickness, and the overall signal-to-noise ratio.

Potential window: The potential window defines the range of applied voltages during electrochemical sensing. To optimize the potential window, we perform the cyclic voltammetry in the range (-1 V to +1 V) and choose the range at which the redox peak is obtained.

Scan rate: The scan rate in cyclic voltammetry controls how fast the potential is swept over the selected range. The scan rate significantly influences the shape and intensity of the redox peaks, as it indicates the electron transfer kinetics and diffusion processes. At slow scan rates, the electron transfer is controlled by diffusion, and the peaks are more pronounced and closer to equilibrium conditions. At faster scan rates, kinetic effects dominate, leading to broadened peaks with higher currents. To optimize the scan rate, we perform CV at different scan rates and study the relationship between peak current and scan rate. Typically, a linear relationship between peak current and the square root of the

scan rate indicates diffusion-controlled processes, while deviations from linearity suggest kinetic limitations. So moderate scan rates are often chosen to balance sensitivity and resolution. For electrochemical sensing of biomolecules, a suitable scan rate might be in the range between 2 to 150 mV/s to achieve high sensitivity while minimizing signal distortion.

Step size (pulse rate): In techniques like differential pulse voltammetry (DPV) and square wave voltammetry (SWV), the step size refers to the increment of potential applied between successive pulses. This parameter influences both the resolution of the peak and the signal-to-noise ratio. Smaller step sizes provide higher resolution but can increase noise, while larger step sizes reduce resolution and may cause overlapping peaks. The optimization of step size is usually challenging. A series of experiments with different step sizes is performed to determine the step size that provides the optimal balance between peak resolution and noise.

2.2 Challenges in achieving high-resolution and specific sample preparation

Some difficulties were faced in the course of my electrochemical sensing study of ascorbic acid, dopamine, and NADH. These difficulties were mostly connected to the achievement of high resolution in voltammetric peaks and problems with sample preparation.

Resolution of voltammetric peaks: The overlapping of voltammetric peaks was one of the primary challenges found throughout the electrochemical sensing procedure, particularly in complex real sample matrices. Attaining high resolution between closely spaced redox potentials of analytes (e.g., NADH, dopamine, uric acid, and glucose) was

challenging due to their similar electrochemical behaviors. This problem decreased the sensitivity and selectivity of the modified electrodes. To overcome this, optimization of the electrode surface modification was performed. By carefully controlling the loading of palladium nanoparticles at Co@NC and the ratio of TCNQ, it was possible to enhance the electron transfer kinetics and selectively interact with the target molecules. This strategy resulted in improved peak separation, which allowed for higher resolution. Additionally, using amperometry and differential pulse voltammetry instead of cyclic voltammetry helped to increase resolution and sensitivity.

Sample Preparation Issues: Real sample analysis in vitamin C tablets, dopamine hydrochloride injection, and avocado juice samples, posed challenges due to the presence of interfering species and matrix effects. These cause inaccurate readings or peak distortions, complicating analyte quantification. To overcome these problems, we employed dilution for dopamine hydrochloride injection, filtration, and dilution techniques for vitamin C tablets, proper dilution ensured that the concentration of ascorbic acid remained within the dynamic range of the sensor. In the case of avocado juice samples, insoluble fibers, and other large molecules were removed using centrifugation followed by filtration, and then dilution and pH adjustment was made to enhance the selective detection of NADH.

2.3 Flow chart of research work

Here, we are presenting a flow chart to illustrate our prospective research work (Figure 2.9). In this flow chart, we initially synthesized our target nanomaterials and their composite, characterized them using various techniques, and assessed their

electrochemical study. Additionally, it has been used for sensing ascorbic acid, dopamine, and NADH biomolecules.

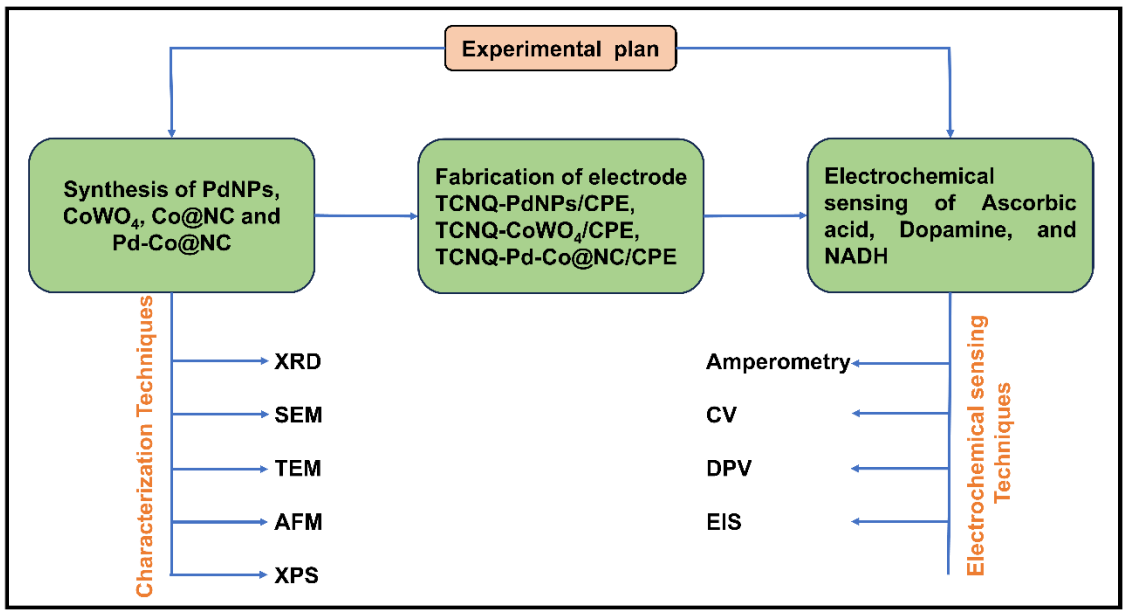

Figure 2.10 Flow chart of research strategy.

2.4 References

[1] C.F. Holder, R.E. Schaak, Tutorial on Powder X-ray Diffraction for Characterizing Nanoscale Materials, ACS Nano 13 (2019) 7359–7365. https://doi.org/10.1021/acsnano.9b05157.

[2] A. Chauhan, Powder XRD Technique and its Applications in Science and Technology, J Anal Bioanal Tech 5 (2014) 1-5. https://doi.org/10.4172/2155-9872.1000212.

[3] R. Sharma, D.P. Bisen, U. Shukla, B.G. Sharma, X-ray diffraction: a powerful method of characterizing nanomaterials, 4 (2012) 77–79. http://recent-science.com/.

[4] E.S. Ameh, A review of basic crystallography and x-ray diffraction applications, International Journal of Advanced Manufacturing Technology 105 (2019) 3289–3302. https://doi.org/10.1007/s00170-019-04508-1.

[5] P. Jagadeesh, S.M. Rangappa, S. Siengchin, Advanced characterization techniques for nanostructured materials in biomedical applications, Advanced Industrial and Engineering Polymer Research 7 (2024) 122–143. https://doi.org/10.1016/j.aiepr.2023.03.002.

[6] M. Suga, S. Asahina, Y. Sakuda, H. Kazumori, H. Nishiyama, T. Nokuo, V. Alfredsson, T. Kjellman, S.M. Stevens, H.S. Cho, M. Cho, L. Han, S. Che, M.W. Anderson, F. Schüth, H. Deng, O.M. Yaghi, Z. Liu, H.Y. Jeong, A. Stein, K. Sakamoto, R. Ryoo, O. Terasaki, Recent progress in scanning electron microscopy for the characterization of fine structural details of nano materials, Progress in Solid State Chemistry 42 (2014) 1–21. https://doi.org/10.1016/j.progsolidstchem.2014.02.001.

[7] A. Mohammed, A. Abdullah, Scanning Electron Microscopy (SEM): A review article Proceedings of the 2018 International Conference on Hydraulics and Pneumatics-Hervex, Băile Govora, Romania. 2018 (2018) 7-9. https://fluidas.ro/hervex/proceedings2018/77-85.

[8] R. Porat, A. Porst, J. Lohse, G. Matke, M. Rebien, The use of integrated Energy (EDX) and Wavelength (WDX) Dispersive X-ray system for defects root cause analysis in an advanced Logic fab IEEE/SEMI Advanced Semiconductor Manufacturing Conference (ASMC) 11 (2010) 123-128. https://doi.org/ 10.1109/ASMC.2010.5551432.

[9] M. Scimeca, S. Bischetti, H.K. Lamsira, R. Bonfiglio, E. Bonanno, Energy dispersive X-ray (EDX) microanalysis: A powerful tool in biomedical research and diagnosis, European Journal of Histochemistry 62 (2018) 89–99. https://doi.org/10.4081/ejh.2018.2841.

[10] R.D. Prasad, R.S. Prasad, R.B. Prasad, S.R. Prasad, S.B. Singha, A.D. Singha, R.J. Prasad, S.B. Teli, P. Sinha, A.K. Vaidya, S. Saxena, U.R. Saxena, A. Harale, M.B. Deshmukh, M.N. Padvi, G.J. Navathe, A Review on Modern Characterization Techniques for Analysis of Nanomaterials and Biomaterials, ES Energy and Environment 23 (2024) 1087. https://doi.org/10.30919/esee1087.

[11] M. Malatesta, Transmission electron microscopy as a powerful tool to investigate the interaction of nanoparticles with subcellular structures, Int J Mol Sci 22 (2021) 12789. https://doi.org/10.3390/ijms222312789.

[12] C.Y. Tang, Z. Yang, Transmission Electron Microscopy (TEM), in: Membrane Characterization, Elsevier Inc., 1 (2017) 145–159. https://doi.org/10.1016/B978-0-444-63776-5.00008-5.

[13] H. Zhang, J. Huang, Y. Wang, R. Liu, X. Huai, J. Jiang, C. Anfuso, Atomic force microscopy for two-dimensional materials: A tutorial review, Opt Commun 406 (2018) 3–17. https://doi.org/10.1016/j.optcom.2017.05.015.

[14] K.W. Shinato, F. Huang, Y. Jin, Principle and application of atomic force microscopy (AFM) for nanoscale investigation of metal corrosion, Corrosion Reviews 38 (2020) 423–432. https://doi.org/10.1515/corrrev-2019-0113.

[15] M.K. Khan, Q.Y. Wang, M.E. Fitzpatrick, Atomic Force Microscopy (AFM) for Materials Characterization, in: Materials Characterization Using Nondestructive Evaluation (NDE) Methods, Elsevier Inc., 8 (2016) 1–16. https://doi.org/10.1016/B978-0-08-100040-3.00001-8.

[16] F.A. Stevie, C.L. Donley, Introduction to x-ray photoelectron spectroscopy, Journal of Vacuum Science & Technology A: Vacuum, Surfaces, and Films 38 (2020) 063204. https://doi.org/10.1116/6.0000412.

[17] E. Mazzotta, S. Rella, A. Turco, C. Malitesta, XPS in development of chemical sensors, RSC Adv 5 (2015) 83164–83186. https://doi.org/10.1039/c5ra14139g.

[18] D.N.G. Krishna, J. Philip, Review on surface-characterization applications of X-ray photoelectron spectroscopy (XPS): Recent developments and challenges, Applied Surface Science Advances 12 (2022) 100332. https://doi.org/10.1016/j.apsadv.2022.

[19] F. Scholz, Voltammetric techniques of analysis: the essentials, ChemTexts 1 (2015) 17. https://doi.org/10.1007/s40828-015-0016-y.

[20] J. P.S., D.S. Sutrave, A Brief Study of Cyclic Voltammetry and Electrochemical Analysis, Int J Chemtech Res 11 (2018) 77–88. https://doi.org/10.20902/ijctr.2018.110911.

[21] N. Elgrishi, K.J. Rountree, B.D. McCarthy, E.S. Rountree, T.T. Eisenhart, J.L. Dempsey, A Practical Beginner's Guide to Cyclic Voltammetry, J Chem Educ 95 (2018) 197–206. https://doi.org/10.1021/acs.jchemed.7b00361.

[22] N.Z.N. Aqmar, W.F.H. Abdullah, Z.M. Zain, S. Rani, Embedded 32-bit Differential Pulse Voltammetry (DPV) Technique for 3-electrode Cell Sensing, in: IOP Conf Ser Mater Sci Eng, Institute of Physics Publishing, 340 (2018) 012016. https://doi.org/10.1088/1757-899X/340/1/012016.

[23] F. Crespi, Differential Pulse Voltammetry: Evolution of an In Vivo Methodology and New Chemical Entries, A Short Review, Journal of New Developments in Chemistry 2 (2020) 20–28. https://doi.org/10.14302/issn.2377-2549.jndc-20-3298.

[24] P. Westbroek, Electrochemical methods, in: Analytical Electrochemistry in Textiles, Elsevier Inc., 37 (2005) 37–69. https://doi.org/10.1533/9781845690878.1.37.

[25] K.J. Samdani, D.W. Joh, M.K. Rath, K.T. Lee, Electrochemical mediatorless detection of norepinephrine based on MoO3 nanowires, Electrochim Acta 252 (2017) 268–274. https://doi.org/10.1016/j.electacta.2017.08.187.

[26] E.P. Randviir, C.E. Banks, Electrochemical impedance spectroscopy: An overview of bioanalytical applications, Analytical Methods 5 (2013) 1098–1115. https://doi.org/10.1039/c3ay26476a.

[27] H.S. Magar, R.Y.A. Hassan, A. Mulchandani, Electrochemical impedance spectroscopy (Eis): Principles, construction, and biosensing applications, Sensors 21 (2021) 6578. https://doi.org/10.3390/s21196578.

[28] A.C. Lazanas, M.I. Prodromidis, Electrochemical Impedance Spectroscopy─A Tutorial, ACS Measurement Science Au 3 (2023) 162–193. https://doi.org/10.1021/acsmeasuresciau.2c00070.